Dual Palmitoylation of PSD-95 Mediates Its Vesiculotubular Sorting, Postsynaptic Targeting, and Ion Channel Clustering✪

Alaa E. El-Husseini,* Sarah E. Craven,* Dane M. Chetkovich,*‡ Bonnie L. Firestein,* Eric Schnell,* Chiye Aoki,§ and David S. Bredt*

*Department of Physiology and ‡Department of Neurology, University of California at San Francisco, San Francisco, California 94143; and §Center for Neural Science, New York University, New York 10003

Abstract. Postsynaptic density-95 (PSD-95/SAP-90) is a palmitoylated peripheral membrane protein that scaffolds ion channels at excitatory synapses. To elucidate mechanisms for postsynaptic ion channel clustering, we analyzed the cellular trafficking of PSD-95. We find that PSD-95 transiently associates with a perinuclear membranous compartment and traffics with vesiculotubular structures, which migrate in a microtubule-dependent manner. Trafficking of PSD-95 with these vesiculotubular structures requires dual palmitoylation, which is specified by five consecutive hydrophobic residues at the NH_2 terminus. Mutations that disrupt dual palmitoylation of PSD-95 block both ion channel clustering by PSD-95 and its synaptic targeting. Replacing the palmitoylated NH_2 terminus of PSD-95 with alternative palmitoylation motifs at either the NH_2 or COOH termini restores ion channel clustering also induces postsynaptic targeting, respectively. In brain, we find that PSD-95 occurs not only at PSDs but also in association with intracellular smooth tubular structures in dendrites and spines. These data imply that PSD-95 is an itinerant vesicular protein; initial targeting of PSD-95 to an intracellular membrane compartment may participate in postsynaptic ion channel clustering by PSD-95.

Key words: PSD • palmitoylation • trafficking • MAGUK • clustering

Introduction

Rapid and efficient neurotransmission requires proper synaptic assembly of signal transducing protein networks. At excitatory synapses, glutamate receptors are clustered at the postsynaptic density (PSD)[1], a thickening of the cytoskeleton beneath the plasma membrane. Also associated with the PSD are cytosolic enzymes including calcium calmodulin-dependent protein kinase II and neuronal nitric oxide synthase that modulate glutamatergic stimuli (Brenman et al., 1996a; Kennedy, 1998).

Although recent studies have helped to define the composition of the PSD (Kornau et al., 1997; Sheng and Wyszynski, 1997; Craven and Bredt, 1998), mechanisms for assembling protein complexes at postsynaptic sites are poorly understood. One attractive candidate is the postsynaptic density protein, PSD-95/SAP-90, a membrane-associated guanylate kinase (MAGUK; Cho et al., 1992; Kistner et al., 1993) that employs PDZ motifs to cluster proteins into complexes at synaptic sites (Kim et al., 1995; Kornau et al., 1995; Brenman et al., 1996a). PSD-95 functions as a molecular scaffold to synaptically anchor Shaker type K^+ channels, *N*-methyl-D-aspartate (NMDA) type glutamate receptors, and associated downstream signaling enzymes (Kornau et al., 1997; Sheng and Wyszynski, 1997; Craven and Bredt, 1998). Genetic analyses have highlighted these roles for MAGUK proteins in synaptic organization and function. Mutations of *discs large* (*dlg*), a MAGUK of *Drosophila*, perturb postsynaptic clustering of a Shaker type K^+ channel at the larval neuromuscular junction (Tejedor et al., 1997). Furthermore, targeted disruption of PSD-95 in mouse alters NMDA receptor mediated synaptic plasticity (Migaud et al., 1998).

Because postsynaptic protein clustering critically participates in both synaptogenesis and plasticity, mechanistic understanding of postsynaptic protein trafficking is an important goal. PSD-95 itself is a valuable tool for studying this protein sorting problem because fluorescently tagged PSD-95-GFP fusion proteins are targeted appropriately to

✪The online version of this article contains supplemental material.

Address correspondence to David S. Bredt, University of California at San Francisco School of Medicine, 513 Parnassus Ave., San Francisco, CA 94143-0444. Tel.: (415) 476-6310. Fax: (415) 476-4929. E-mail: bredt@itsa.ucsf.edu

[1]*Abbreviations used in this paper*: BFA, brefeldin A; dlg, discs large; GAP-43, growth associated protein-43; GFP, green fluorescent protein; MAGUK, membrane-associated guanylate kinase; NMDA, *N*-methyl-D-aspartate; PDZ, postsynaptic density-95, discs large, zonula occludens; PSD, postsynaptic density.

the PSD (Arnold and Clapham, 1999; Craven et al., 1999). Taking advantage of this model, recent work shows that postsynaptic clustering of PSD-95 in hippocampal neurons critically relies on three structural features: the palmitoylated NH_2 terminus, the first and second PDZ domains, and a synaptic targeting motif within the COOH-terminal 25 amino acids (Craven et al., 1999). How these molecular features of PSD-95 mediate postsynaptic clustering remains unknown.

Some insight into mechanisms for protein sorting in neurons has been gained by comparison with polarized protein targeting in epithelial cells. Many transmembrane proteins that occur along the basolateral surface of epithelial cells have a somatodendritic or postsynaptic distribution in neurons whereas apical proteins of epithelial cells are typically found in neuronal axons (Dotti and Simons, 1990; Jareb and Banker, 1998; Rongo et al., 1998). Cellular analyses of epithelia have determined that targeting of transmembrane proteins to either the apical or basolateral membrane occurs in sorting endosomal compartments (Trowbridge et al., 1993). It is unclear whether similar sorting compartments mediate postsynaptic clustering in neurons or whether this type of processing would apply at all to a palmitoylated peripheral membrane protein, like PSD-95.

To clarify mechanisms for postsynaptic sorting and assembly of postsynaptic proteins, we have evaluated subcellular trafficking of fluorescently labeled PSD-95 proteins. Strikingly, we find that PSD-95 is sorted with perinuclear vesicles in both heterologous cells and in developing neurons. When visualized in living cells, PSD-95 positive vesicles migrate to and from perinuclear vesicles and this movement requires intact microtubules. Site-directed mutagenesis demonstrates that perinuclear vesicular sorting and ion channel clustering of PSD-95 in heterologous cells and its postsynaptic targeting in neurons all rely on dual palmitoylation of cysteines 3 and 5, and that the yet unidentified palmitoyltransferase responsible for this modification recognizes a consensus of 5 consecutive hydrophobic amino acids. Replacing the palmitoylated NH_2 terminus of PSD-95 with alternative palmitoylation motifs at either the NH_2 or COOH terminus restores ion channel clustering and postsynaptic targeting. These data imply that PSD-95 is not merely a static cytoskeletal element but that PSD-95 is an itinerant vesicular protein and that initial targeting of PSD-95 to an intracellular membrane compartment may participate in postsynaptic ion channel clustering by PSD-95.

Materials and Methods

Antibodies

The following antibodies were used: rabbit polyclonal antibodies to $K_v1.4$ (Kim et al., 1995), PSD-95 (Brenman et al., 1996b), and NR2B (Zymed) and monoclonal antibodies to PSD-95 (#046; Affinity Bioreagents), NR1 (PharMingen), GFP (Quantum, Clontech), HA epitope tag (BABCO), and FLAG epitope tag (Kodak). Dr. Frances Brodsky (University of California San Francisco) kindly provided rabbit polyclonal antibodies to Golgi 58K (TGN-38), and to the cation-independent mannose-6-phosphate-receptor (CI-M6PR). Monoclonal antibodies to E-cadherin and to the apical marker, gp-135, were gifts from Dr. Keith Mostov (University of California San Francisco).

cDNA Cloning and Mutagenesis

Subcloning of wild-type cysteine mutant forms of PSD-95 as NH_2-terminal fusions with GFP (PSD-95 GFP, C35S, C3S, and C5S), in pGW1 were previously described (Topinka and Bredt, 1998; Craven et al., 1999). NH_2-terminal deletion mutants of PSD-95 were generated by PCR and subcloned into the HindIII and EcoRI of GW1. All of the point mutations at the NH_2-terminal region of PSD-95 derived from full-length PSD-95-GFP in GW1 as described below. PCR was first used to introduce a silent mutation within the codon encoding amino acid 14 to create a unique KpnI. Oligonucleotides encoding the first 13 amino acids of PSD-95 containing the described point mutations were then subcloned into the HindIII-KpnI sites. GAP-43 GFP full-length and mutant forms were generated by PCR and subcloned into the HindIII and Kpn1 sites in frame and in front of GFP in a GFP/GW1 construct described previously (Craven et al., 1999). PSD-95 paralemmin COOH terminus fusion protein (PSD-95/Parlm) was generated by inserting the last 12 amino acids of paralemmin (Kutzleb et al., 1998) on the COOH terminus of GFP of the PSD-95:C3,5S construct. Proper introduction of all mutations was verified by DNA sequencing.

Cell Transfection and Metabolic Labeling

COS7, HEK-293 and MDCK cells were grown in Dulbecco's modified Eagle's medium (DMEM) containing 10% fetal bovine serum, penicillin, and streptomycin. PC12 cells used the same media containing 5% fetal bovine serum and 10% horse serum and were differentiated for 3 d after transfection in media containing 50 ng/ml NGF. Cells were transfected using Lipofectamine reagent according to the manufacturer's protocol (Gibco). Stable MDCK cells were generated by cotransfecting a PSD-95 expression construct in a GW1 vector together with pcDNAIII and selecting for stable transformants with 1 mg/ml G418. To form polarized monolayers, MDCK cells were plated on 0.4 mm diameter Transwells™ (Corning Costar) and grown for 2–3 d. For studies of palmitoylation, metabolic labeling of transfected COS7 cells was done as previously described (Topinka and Bredt, 1998).

Transfection of Primary Neuronal Cultures and Immunofluorescent Labeling

Hippocampal cultures were transfected as previously described (Craven et al., 1999). In brief, acutely dissociated hippocampal neurons from E18 rats were transfected in suspension by lipid-mediated gene transfer. Cells were then plated at a density of 600 cells/mm^2 on glass coverslips (Fisher) and maintained in Neurobasal media (Gibco) supplemented with B27. Coverslips were removed from culture wells and processed for immunofluorescence or GFP as previously described (Craven et al., 1999). Images were taken under fluorescence microscopy with a 100× oil-immersion objective (NA = 1.4) affixed to a Leica upright microscope. Confocal microscopy used a Krypton-Argon laser and a BioRad MRC 1024 equipped with a 63× 1.4 NA oil-immersion objective. Vertical images were reconstructed from 10 consecutive horizontal sections taken with the motor step size set at 1 μm.

Electron Microscopic Immunocytochemistry

Adult rats were fixed by transcardial perfusion with a phosphate-buffered aldehyde mixture, consisting of 4% paraformaldehyde and 3% acrolein or 2.5% glutaraldehyde. Sections were prepared (40 μm) and blocked in saline buffered with 0.01 M phosphate (PBS) containing 1% BSA. After an overnight incubation with affinity-purified anti-PSD-95 antibody (1 μg/ml), sections were processed for pre-embedding colloidal gold immunolabeling, using 1-nm gold conjugated anti-rabbit IgG as the label. A silver intensification kit (Amersham) was then used to enlarge the 1-nm gold particles to >5 nm for light and electron microscopic detection (Chan et al., 1990). These sections were post-fixed with 1% glutaraldehyde, then with 1% osmium tetroxide, and stained en bloc with 4% uranyl acetate. Sections were dehydrated for infiltration with EMBED 812 resin (EM Sciences) and ultrathin sections (80 nm) were examined without counterstaining. Post-embedding colloidal gold labeling was achieved as described (Aoki et al., 1999b). The 1-nm gold conjugated anti–rabbit IgG was purchased from Goldmark, and the silver-intensification kit was from Amersham.

Imaging of PSD-95 GFP in Live Cells

5 h after transfection, COS7 cells on glass coverslips were placed into a Bioptechs culture dish heated to 37°C. Images were acquired (100-ms ex-

posure) every 30 seconds for 30–180 min with excitation at 470/40 nm and emission at 525/50 nm. Imaging was done using a Zeiss Axiovert S100 TV inverted microscope equipped with a C-Apochromat (NA = 1.2) 63× water objective, a Hamamatsu 12-bit ORCA interline CCD camera, a Sutter excitation and emission filter-wheel and a Universal Imaging Corporation MetaMorph Imaging system.

Supplemental Online Material

Video 1. Visualization of transport intermediates of PSD-95.
Video 2. PSD-95 is trafficked with vesiculotubular structures that accumulate in a perinuclear domain.
Video 3. Nocodazole treatment paralyzes transport intermediates of PSD-95.
Video 4. NH_2-terminal palmitoylation is required for sorting of PSD-95 to the perinuclear vesicular domain.
Videos 5–7. Ion channel clustering by PSD-95 appears to involve vesiculotubular trafficking. COS cells transfected with PSD-95 GFP and Kv1.4 were monitored over time for GFP.

All videos are available at http://www.jcb.org/cgi/content/full/148/1/159/DC1.

Results

PSD-95 Is Sorted with Perinuclear Vesicles in Heterologous Cells and in Neurons

To define cellular processes that mediate postsynaptic ion channel clustering by PSD-95, we first analyzed the subcellular distribution of exogenous PSD-95 expressed in various cell lines. 12 h after transfection of COS cells, wild-type or tagged versions of PSD-95 occur diffusely throughout the cytoplasm but are also conspicuously concentrated at a perinuclear compartment (Fig. 1 A, top). The accumulation of fluorescent PSD-95 at this perinuclear region steadily progresses from 5–8 h after transfection (see time lapse below). To determine whether this transient perinuclear localization of PSD-95 corresponds to a specific organelle, transfected cells were double-stained for PSD-95 and either the mannose-6-phosphate receptor, Golgi 58K, TGN38, or DND-99 (Lysotracker). The perinuclear localization of PSD-95 corresponds to that of the mannose 6-phosphate receptor (M6PR; Fig. 1, B and C), a well-characterized marker of late endosomes (Griffiths et al., 1988). PSD-95 localization only partially overlaps that of the Golgi markers, Golgi 58K, and TGN38; PSD-95 does not overlap at all with the lysosomal marker DND-99 (Fig. 1 B and data not shown).

As found in COS cells, PSD-95 expressed in either HEK293 or PC12 cells also coincides with the M6PR positive compartment (Fig. 1 A, bottom, and data not shown). Furthermore, in developing hippocampal neurons we find that transfected PSD-95 GFP (not shown) and endogenous PSD-95 (Fig. 2) transiently colocalize with the M6PR during the first 2 d in culture. A similar perinuclear localization is observed for NMDA receptor subunits NR1 and NR2B (Fig. 2). By contrast, the microtubule-associated protein, MAP2, occurs in developing neurites and is not concentrated in the perinuclear domain. As the neurons mature, PSD-95 becomes less concentrated in this perinuclear domain and begins to accumulate in small clusters along the processes (Fig. 2).

Accumulation of PSD-95 at the Perinuclear Domain Is Brefeldin A- and Nocodazole-sensitive

To help to determine whether sorting of PSD-95 to the perinuclear domain requires active vesicular trafficking, we treated PSD-95–expressing heterologous cells with BFA. BFA has multiple and diverse effects on vesicular trafficking in cells including disassembly of the Golgi complex (Lippincott-Schwartz et al., 1991). 2 h after transfection, before PSD-95 accumulates in the perinuclear compartment, treatment with BFA completely prevents the accumulation of PSD-95 (Fig. 3 A); instead PSD-95 protein occurs diffusely throughout the cytoplasm. However, addition of BFA after the perinuclear accumulation of PSD-95 does not alter the localization of PSD-95 or its colocalization with M6PR even after prolonged (8 h) treatment (data not shown). These results indicate that accumulation of PSD-95 depends on trafficking through the secretory pathway, but that the perinuclear vesicular domain that PSD-95 resides in is a compartment distinct from the Golgi complex. In contrast, nocodazole, which depolymerizes microtubules and not only disperses Golgi-derived tubules but also endosomes (Cole et al., 1996), blocks accumulation of PSD-95 at the perinuclear compartment and disperses both PSD-95 and the M6PR to similar vesicular structures within the cell (Fig. 3 A). These results suggest that PSD-95 accumulates in a perinuclear endosomal compartment rather than in the Golgi complex.

PSD-95 GFP Is Trafficked through Pleomorphic Vesiculotubular Structures

We used video microscopy to monitor the dynamics of PSD-95-GFP trafficking in live COS cells starting 5 h after transfection. During the first hour, vesicles and tubular structures are constantly forming and moving towards the plasma membrane as well as to the perinuclear region (see video 1). 1–3 hours later, accumulation of PSD-95 GFP in the perinuclear region becomes obvious and the accumulated PSD-95 GFP persists for the remainder of the imaging period (videos 1 and 2). Pleomorphic tubular structures, rather than small vesicles, are the primary vehicles for the transport of PSD-95 GFP. Fig. 3 D shows examples of the various vesicular and tubular structures containing PSD-95 GFP observed 6 h after transfection. These structures undergo dynamic shape changes as they move along tracks (possibly microtubules) to the cell periphery and to the perinuclear region. Some of these vesicular structures fuse with the plasma membrane. We also observed that tubular elements containing PSD-95 GFP typically undergo dramatic shape changes during their movement. These transport intermediates often bifurcate and show elastic properties, including extension and retraction during movement. Moving tubules undergo continuous budding, translocation, and fusion with other transport intermediates carrying PSD-95 GFP to the plasma membrane or to the perinuclear region. These properties are similar to the trafficking of Golgi-derived vesicular transport intermediates for transmembrane proteins (Sciaky et al., 1997). Acute addition of nocodazole completely paralyzes PSD-95 transport intermediates, indicating that their movement requires microtubule-mediated transport (video 3).

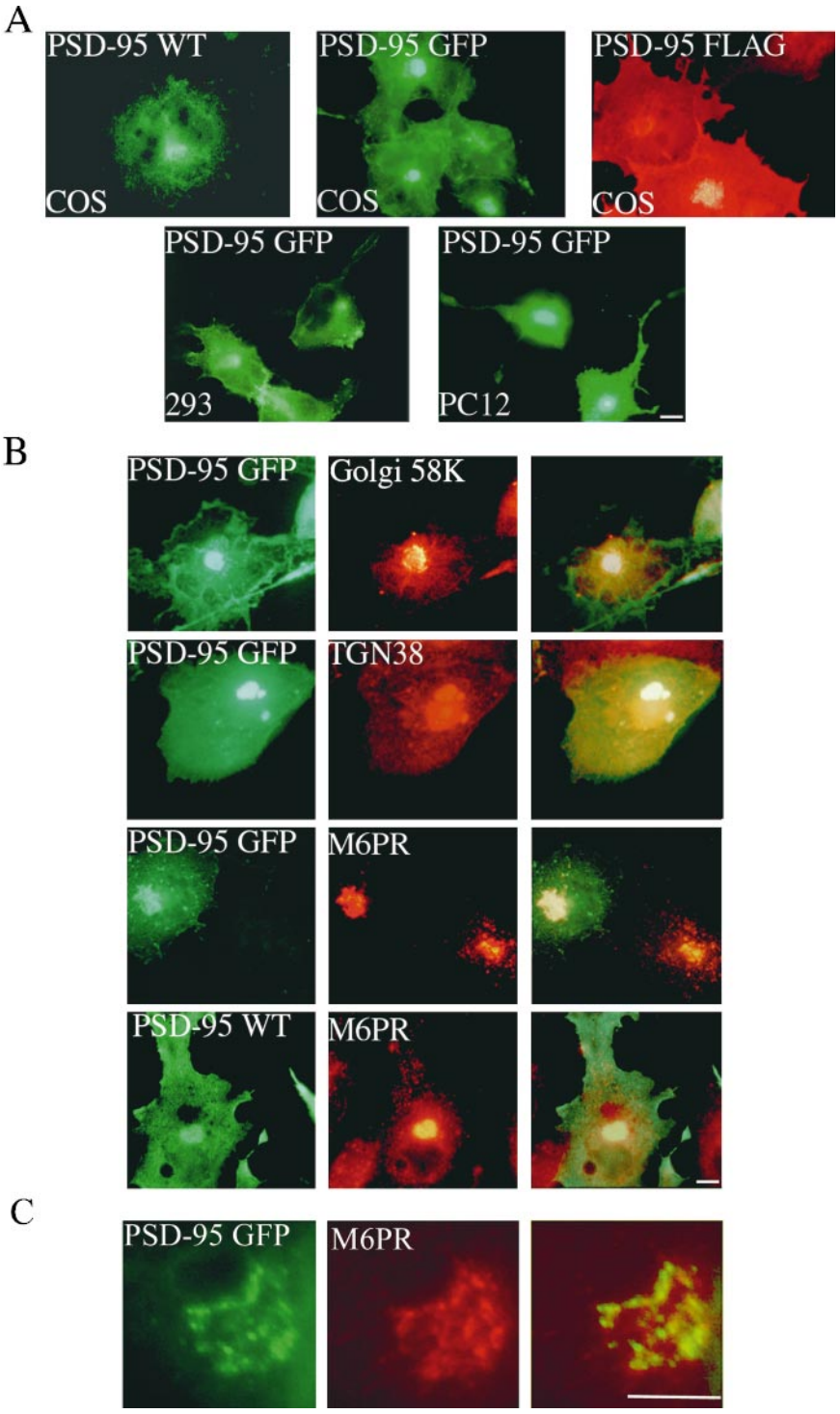

Figure 1. PSD-95 is sorted to a vesicular perinuclear domain. (A) Exogenous PSD-95 accumulates at a perinuclear domain in transfected COS (top), HEK-293 and PC12 cells (bottom). Cells were transfected with either wild-type PSD-95 (PSD-95 WT) or PSD-95 fused to GFP (PSD-95 GFP) or FLAG-epitope tag (PSD-95 FLAG). (B) In COS cells, perinuclear staining for PSD-95 (green) partially overlaps with a Golgi marker Golgi 58K (red) and with a trans-Golgi marker TGN-38 (red), but extensively colocalizes with a late endosomal marker, mannose-6-phosphate receptor (red; M6PR). (C) High magnification shows colocalization of PSD-95 with M6PR. Merged images are shown in the right panels for B and C. Bars, 10 μm.

PSD-95 Localizes to Intracellular Membranes and to the PSD in Cortical Neurons

To determine whether PSD-95 also associates with membranous intracellular structures of neurons within intact brain, we performed electron microscopic immunocytochemical staining of the rat cerebral cortex, using a well characterized anti–PSD-95 antiserum (Brenman et al., 1996a) and established methods for immunocytochemical staining (Aoki et al., 1999b). Previous ultrastructural studies of PSD-95 in forebrain have been limited to a few studies focusing on the localization of PSD-95 at PSDs (Hunt et al., 1996; Aoki et al., 1998; Valtschanoff et al., 1999). Consistent with that work, we have found using the post-embedding gold method that labeling for PSD-95 occurs at the PSDs of >89% of cortical synapses (Aoki et al., 1999a). However, we also find, using a silver-intensified

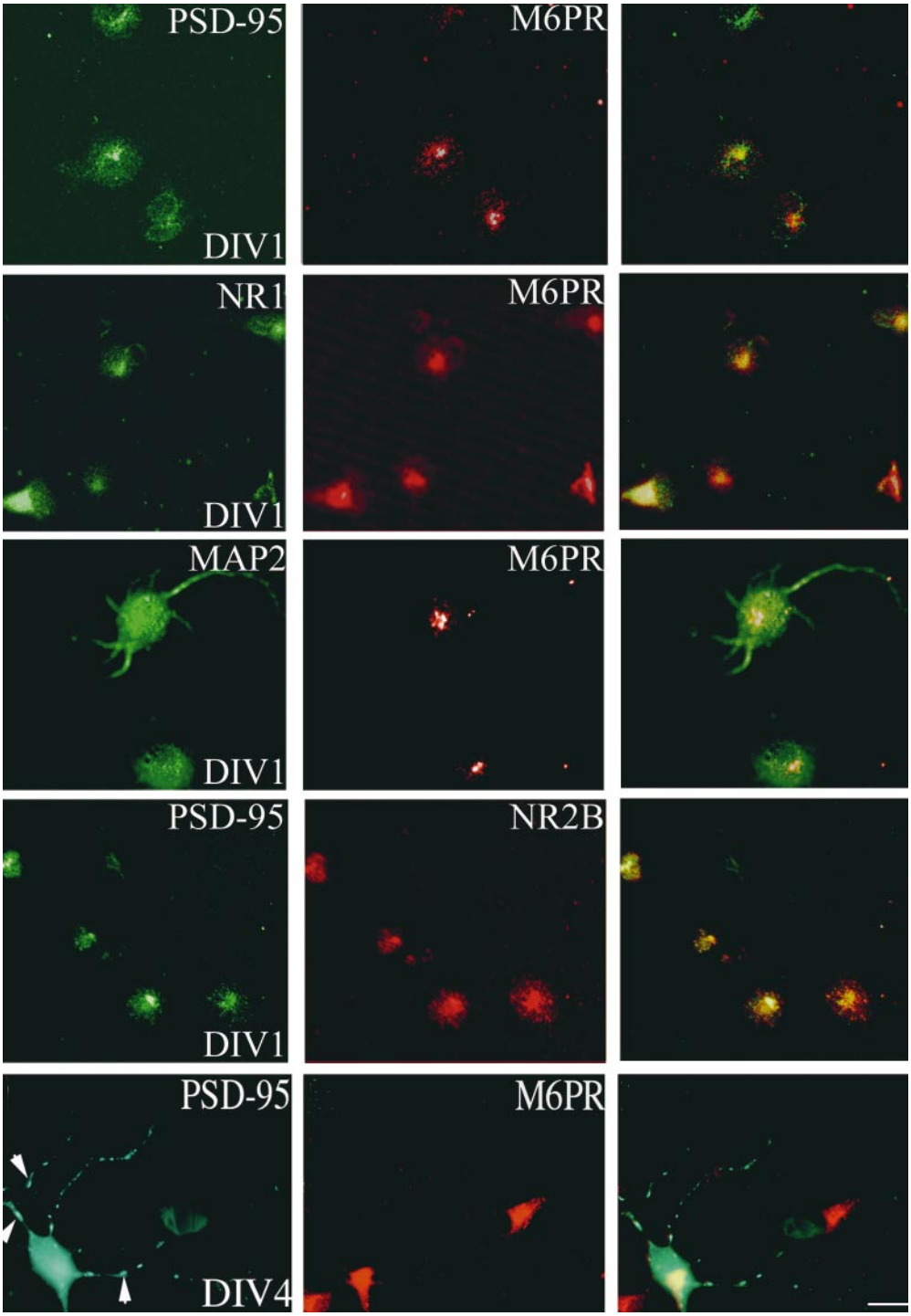

Figure 2. Accumulation of PSD-95 at a perinuclear domain precedes dendritic clustering in primary hippocampal neurons. Endogenous PSD-95 expression in developing hippocampal neurons is shown at 1 d (DIV1) and 4 d (DIV4) in vitro. The expression pattern of PSD-95 (green) is compared with the endosomal marker M6PR (red) and merged images are shown in the right panels. At DIV1, PSD-95 shows strong perinuclear staining that coincides with M6PR. NMDA receptor subunits, NR1 and NR2B, colocalize with PSD-95 and M6PR at DIV1 whereas MAP2 shows diffuse staining in the soma and processes. By DIV4, PSD-95 occurs diffusely in the soma, and at this stage clusters begin to form in the neurites (arrowheads). Bar, 10 μm.

gold pre-embedding method (Chan et al., 1990), that PSD-95 localizes to nonsynaptic sites (Fig. 4 A) and is often found in association with the cytosolic surface of membranous intracellular structures. Fig. 4 B shows an example of PSD-95 immunoreactivity associated with intracellular smooth endoplasmic reticulum in a dendritic shaft of a cortical neuron. In a nearby synaptic spine PSD-95 immunoreactivity is associated with the spine apparatus adjacent to an unlabeled PSD of an asymmetric synapse (Fig. 4 B).

Vesicular Sorting of PSD-95 Requires a Short NH_2-terminal Palmitoylated Motif

We next determined the region(s) of PSD-95 sufficient for its association with the perinuclear vesicular domain. We first transfected COS cells with a series of progressively larger deletion constructs encoding PSD-95 fused to GFP. This deletion analysis showed that a construct containing the first nine amino acids of PSD-95 fused to GFP occurs diffusely when expressed in COS cells, whereas constructs

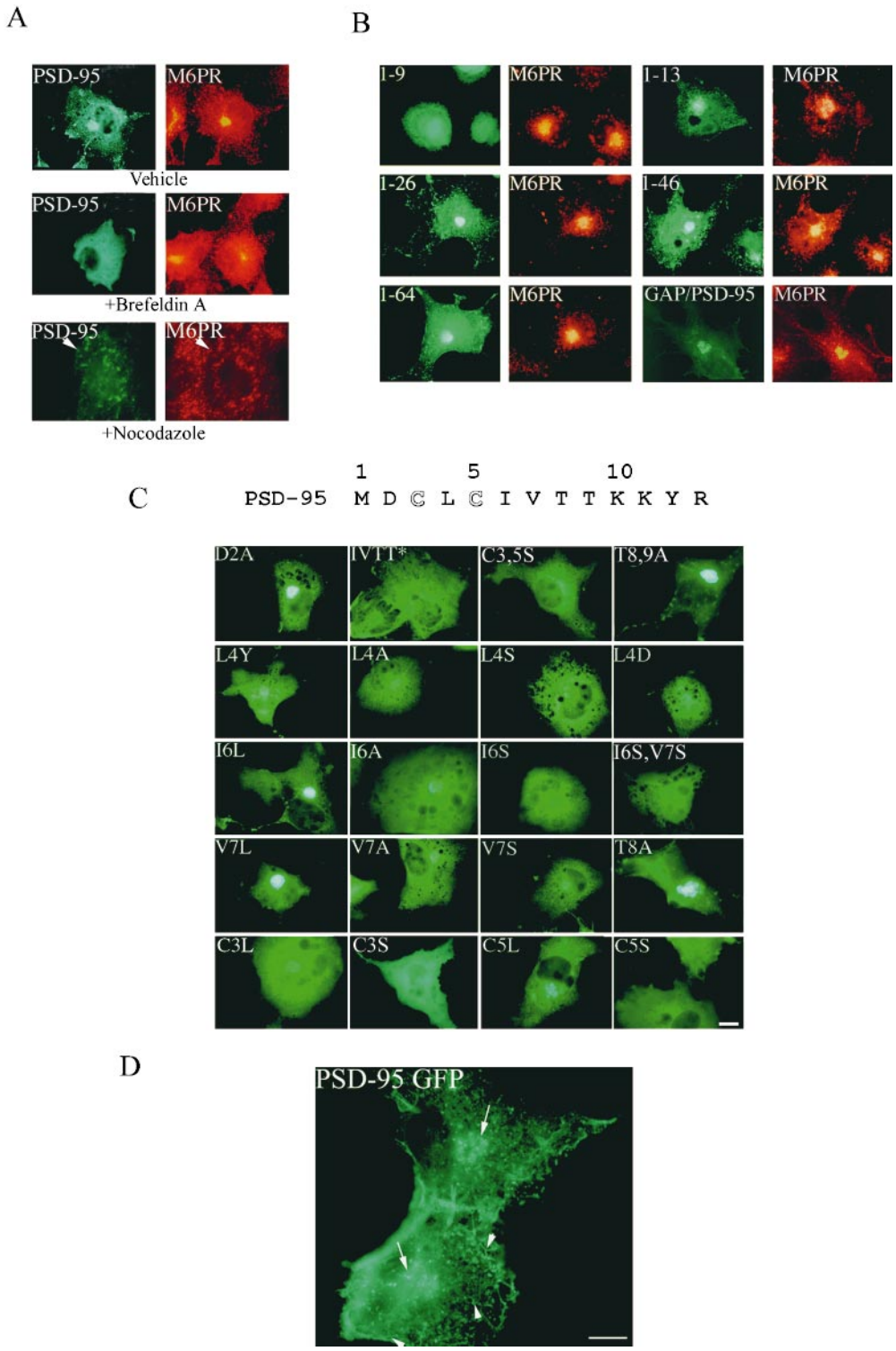

Figure 3. Perinuclear accumulation of PSD-95 relies on the palmitoylation motif and requires a functional secretory pathway and intact microtubules. (A) COS cells were transfected with PSD-95. 2 h after transfection, cells treated for 7 h with either vehicle or 10 μg/ml BFA, or 20 μg/ml nocodazole and were examined 8 h later for PSD-95 (green) and M6PR (red). For the nocodazole-treated cells, arrowheads point to the single cell in the field transfected with PSD-95 (bottom). (B) Targeting of PSD-95 to a M6PR-positive perinuclear compartment is mediated by an NH_2-terminal palmitoylated motif. Amino acids 1–13 but not 1–9 are sufficient for targeting GFP to the perinuclear, M6PR-positive compartment. Perinuclear accumulation is also observed with GFP-fusion constructs containing amino acids 1–26, 1–46, and 1–64. A chimera containing the first 12 amino acids of GAP-43 fused PSD-95 (GAP/PSD-95) is also sorted to the perinuclear domain. (C) Mutations in the palmitoylation motif dramatically affect perinuclear vesicular sorting. Mutations of Cys3 and/or 5 to Ser (C3,5S, C3S, C5S) or amino acids 6-9 (IVTT) to TEIN (denoted as IVTT*) disrupt vesicular sorting, whereas mutations of amino acids 2, 8, or 9 to Ala (D2A; T8A and T89A) do not. All mutations of amino acid 4 (L4Y, L4A, L4S, and L4D) dramatically alter sorting to the perinuclear domain, with the more hydrophilic changes being more significant. Mutations of amino acids 6 and 7 to hydrophobic ones maintain normal sorting (I6L, V7L), whereas mutating either Cys3 or Cys5 to Leu only partially maintains the perinuclear distribution (C3L, C5L). (D) An enlarged image shows in greater detail the localization of PSD-95 along vesiculotubular structures that resemble Golgi-derived tubules (arrowheads) and also to a perinuclear region (arrows). Bar, 10 μm.

containing the first 13, 26, 46, or 64 amino acids all transiently accumulate at the perinuclear domain, just like full-length PSD-95 (Fig. 3 B).

To determine whether association of PSD-95 with perinuclear vesicles requires NH_2-terminal palmitoylation, we evaluated the distribution of palmitoylation-deficient mutants. Mutation of cysteine 3 or 5 of PSD-95 to serine prevents palmitoylation (Topinka and Bredt, 1998), and these mutations completely disrupt vesicular sorting of PSD-95 in COS cells (Fig. 3 C). Instead, the palmitoylation-deficient mutants occur diffusely throughout the cells. To determine if a dually palmitoylated motif is sufficient for

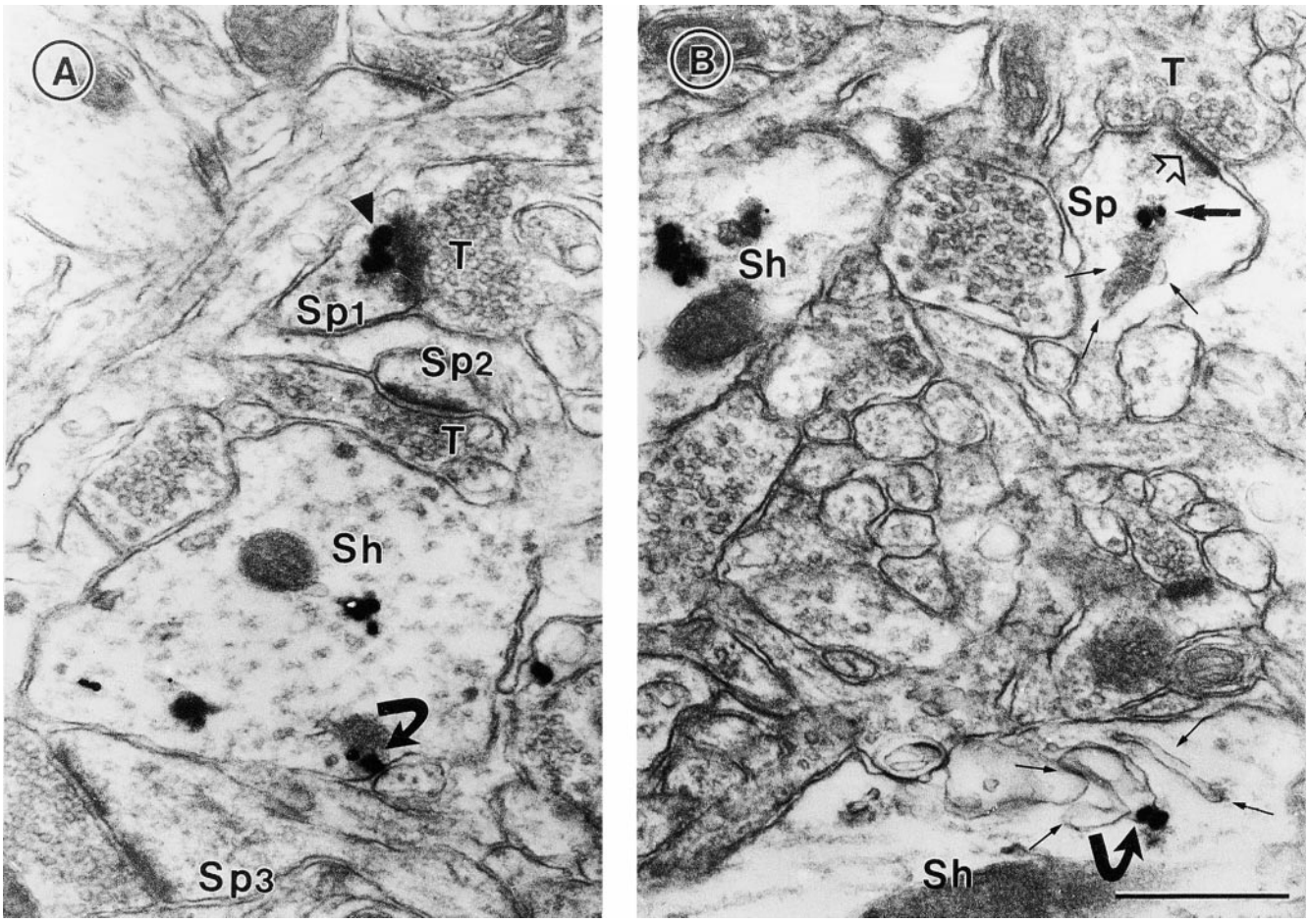

Figure 4. Ultrastructural localization of PSD-95 at synaptic and nonsynaptic sites. The silver-intensified colloidal gold (SIG) method was used for electron micrographic immunolabeling of PSD-95 in visual cortex. (A) Gold particles are associated with the PSD within a spine (arrowhead in Sp1) that opposes an unlabeled terminal, T. Two other spines (Sp2 and Sp3) are without SIG immunolabeling. Within the dendritic shaft (Sh), immunoreactivity is associated with the plasma membrane (curved arrow) and elsewhere. (B) Within a dendritic spine (Sp) of an asymmetric synapse, PSD-95 (dark arrow) is associated with the spine apparatus (three fine arrows). The open arrow points to the unlabeled postsynaptic density. In a dendritic shaft below (Sh), SIG label (curved arrow) is associated with a complex of smooth ER (four fine arrows). Another shaft, to the left of Sp, exhibits immunoreactivity in the cytoplasm, as is shown in A. Bar, 500 nm.

vesicular trafficking of PSD-95, we replaced amino acids 1–13 of PSD-95 with the first 12 amino acids of growth-associated protein-43 (GAP-43), another dually palmitoylated motif. Indeed, this chimeric protein (GAP/PSD-95) was efficiently palmitoylated (Fig. 5 D) and trafficked to the same perinuclear compartment as wild-type PSD-95 (Fig. 3 B).

Palmitoylation of PSD-95 Is Determined by a Hydrophobic Consensus Sequence

To analyze further palmitoylation of PSD-95, we determined the structural requirements for this protein lipidation. As shown in Fig. 5 B, constructs containing at least the first 13 amino acids of PSD-95 are efficiently palmitoylated, whereas a construct containing only the first 9 amino acids is not detectably palmitoylated. These data indicate that the palmitoyltransferase that modifies PSD-95 recognizes a short sequence confined to the NH_2 terminus. This short consensus need not occur at the extreme NH_2 terminus, as insertion of 6 amino acids (VSKSGS) between the starter methionine and the palmitoylated cysteines does not influence the efficacy of palmitoylation (Fig. 5 B).

We further dissected the sequence requirements within the first 13 amino acids. Mutating amino acids 10–13 partially attenuates palmitoylation efficiency whereas mutating amino acids 6–9 almost completely abolishes palmitoylation (Fig. 5, B and D). We next generated a series of constructs in which we individually mutated amino acids 2–9 of PSD-95 to alanine and evaluated [^{3}H]palmitate labeling in transfected cells. Changing amino acids 4-Leu, 6-Ile or 7-Val to alanine significantly reduces or eliminates palmitoylation, but mutations of 2-Asp, 8-Thr, or 9-Thr has no effect (Fig. 5 C, and data not shown). These data indicate that mutations of the hydrophobic amino acids disrupt palmitoylation, whereas mutations of hydrophilic amino acids do not. To investigate this further, we individually mutated amino acids 6-Ile and 7-Val to either serine, a hydrophilic amino acid, or to leucine, a hydrophobic amino acid. Both serine mutants are weakly palmitoylated

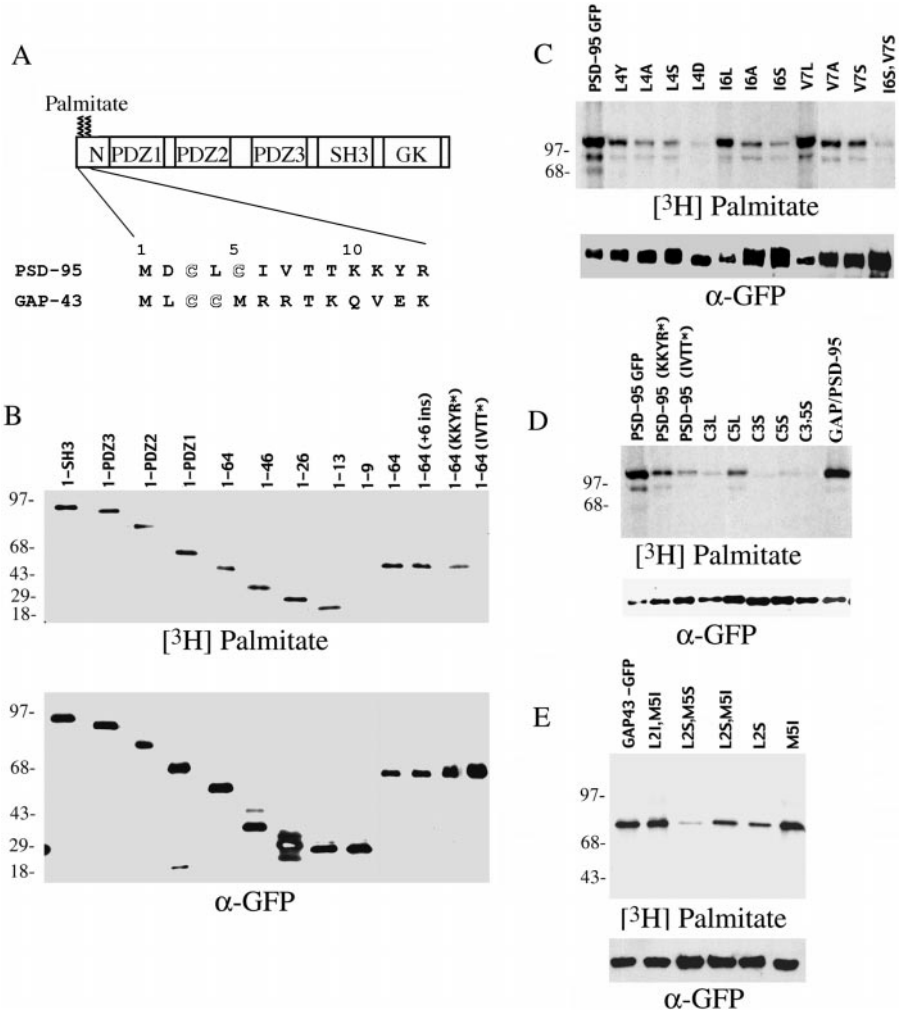

Figure 5. Palmitoylation of PSD-95 and GAP-43 are determined by consensus sequences of 5 consecutive hydrophobic amino acids. (A) Schematic illustration of the domain structure of PSD-95 and sequence alignment of the NH_2 terminus of PSD-95 with GAP-43. (B) Analysis of PSD-95 deletion mutants shows that amino acids 1–13 are sufficient for efficient palmitoylation. Mutations of amino acids 6–9 (IVTT to TEIN; IVTT*) have a more dramatic effect on protein palmitoylation than changing amino acids 10–13 (KKYR to NIFS; KKYR*). Insertion of 6 amino acids (VSKSGS) after the starter Met (+6 ins) does not alter palmitoylation. (C) Site-directed mutational analysis of PSD-95 shows that palmitoylation requires hydrophobic amino acids at positions 4, 6, and 7 (see text for detailed analysis). (D) Mutating Cys3 or 5 to Ser blocks palmitoylation whereas changing these residues to Leu partially maintains palmitoylation (C3L, C5L). A chimera containing the first 12 amino acids of GAP-43 fused to PSD-95 (GAP/PSD-95) is efficiently palmitoylated. (E) Hydrophilic, but not hydrophobic, mutations of the residues (Leu-2 and Met-5) surrounding Cys3 and Cys4 of GAP-43 reduce its palmitoylation (see text for detailed analysis).

(Fig. 5 C) whereas the leucine mutants are robustly palmitoylated (Fig. 5 C). Mutation of amino acid 4 from leucine to either aspartate or serine also disrupts palmitoylation, whereas mutation to the less hydrophilic amino acid tyrosine partially preserves palmitoylation (Fig. 5 C).

Previous studies showed that mutating cysteine 3 or 5 to serine completely disrupts palmitoylation (Topinka and Bredt, 1998). That both Cys→Ser mutants are not palmitoylated might now be explained by a requirement of the palmitoyltransferase for a hydrophobic consensus. This interpretation would predict that mutating cysteine 3 or 5 (which themselves are hydrophobic) to another hydrophobic amino acid would preserve palmitoylation of the remaining cysteine. Indeed, we found that Cys3Leu and Cys5Leu mutants show residual palmitoylation that amount to ~20 and ~40% of the wild-type level, respectively (Fig. 5 D). Taken together, these data imply that palmitoylation of PSD-95 is mediated by a short NH_2-terminal consensus sequence that critically relies on five consecutive hydrophobic amino acids (Cys-Leu-Cys-Ile-Val).

To determine whether a similar hydrophobic consensus might determine NH_2-terminal palmitoylation of other proteins, we evaluated GAP-43, whose site of palmitoylation also contains five consecutive hydrophobic amino acids (Met-Leu-Cys-Cys-Met) (Liu et al., 1993). As found for PSD-95, palmitoylation of GAP-43 is reduced by mutating a hydrophobic amino acid adjacent to the cysteines (Leu-2) to serine. Furthermore, mutating both Leu-2 and Met-5 of GAP-43 to serine nearly abolishes palmitoylation (Fig. 5 E). On the other hand, palmitoylation is preserved if Leu-2 and Met-5 are mutated to a hydrophobic amino acid (Ile). Thus, palmitoylation of both PSD-95 and GAP-43 appear to be specified by five consecutive hydrophobic amino acids.

To evaluate further the role of palmitoylation in vesicular sorting of PSD-95, we monitored the trafficking of each NH_2-terminal mutant of PSD-95 in transfected COS cells. We found that all mutations that dramatically reduce protein palmitoylation (Cys3,5Ser, Cys3Ser, Cys5Ser, Leu4Ser, Leu4Asp, and Ile6Ser, Val7Ser) also block accumulation of PSD-95 at the perinuclear compartment (Fig. 3 C). Conversely, PSD-95 occurs normally at the perinuclear domain in transfections with mutants that preserve palmitoylation (Asp2Ala, Ile6Leu, Val7Leu, Thr8Ala, and Thr8,9Ala) (Fig. 3 C). For mutants that have reduced efficiency of palmitoylation (Leu4Tyr, Leu4Ala, Cys3Leu, Cys5Leu, Ile6Ala, Val7Ala, and Val7Ser), the density of PSD-95 at the perinuclear domain decreases but remains apparent above the diffuse level in the cytosol (Fig. 3 C).

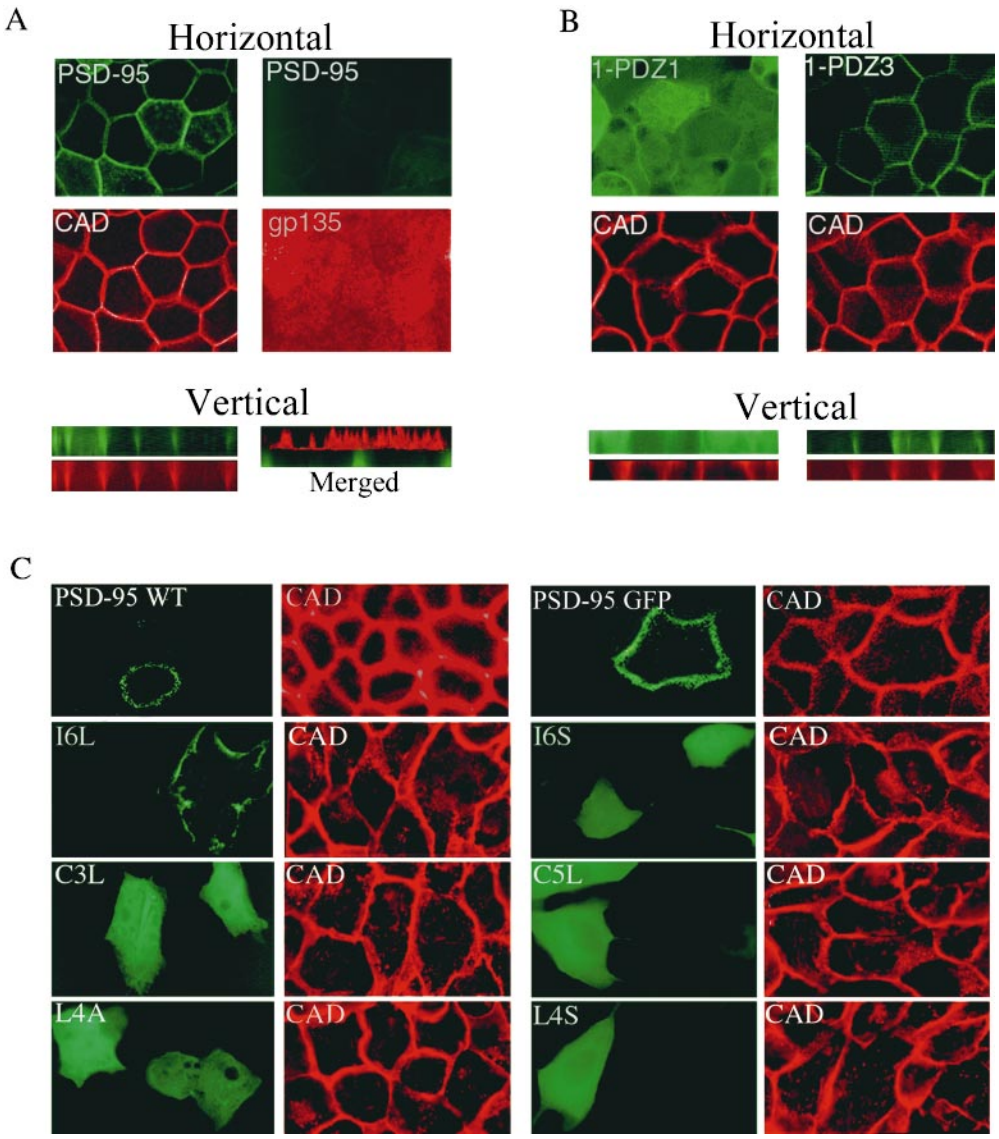

Figure 6. Sorting of PSD-95 to the basolateral membrane of polarized epithelial cells requires protein palmitoylation and PDZ domains. (A) In a horizontal optical section (A, top left pair) stably transfected PSD-95 (green) colocalizes with E-cadherin (CAD, red) along the lateral plasma membranes in polarized MDCK cells. PSD-95 (green) and CAD (red) colocalize along the basolateral membranes in a vertical section (A, bottom left pair). PSD-95 (green) does not occur in an apical horizontal section which is positive for the apical marker gp135 (red). A merged vertical section shows that PSD-95 (green) occurs along the basolateral membranes whereas gp135 (red) is confined to the apical membrane. Cells were investigated by confocal fluorescence microscopy and three-dimensional reconstruction. (B) A stably transfected NH_2-terminal mutant of PSD-95 containing all three PDZ domains (1-PDZ3) is sorted to the basolateral membrane whereas a construct extending through only the first PDZ domain (1-PDZ1) occurs diffusely in the cytosol. Horizontal optical sections at the level of the tight junctions and reconstructed vertical sections are shown. (C) Distribution of wild-type and mutants forms of PSD-95, including I6L, I6S, C3L, C5L, L4A, and L4S in transiently transfected MDCK cells. All of the PSD-95 mutant forms, except for I6L, are expressed diffusely in these cells. The mutant form I6L, which maintains palmitoylation, colocalizes with the basolateral marker E-cadherin.

We also examined the trafficking of a mutant form of PSD-95, Ile6Ser in live cells. This single amino acid change in PSD-95 dramatically reduces its palmitoylation and prevents its vesicular sorting. Imaging of live cells expressing this point mutant form of PSD-95 fails to show formation of any vesicular structures (video 4). Instead, diffuse cytoplasmic GFP signal is seen throughout the recording period.

Basolateral Sorting of PSD-95 in Polarized Epithelial Cells Requires Dual Palmitoylation

The cellular pathways for dendritic and for postsynaptic sorting of certain neuronal transmembrane proteins share features with protein targeting to the basolateral membrane of polarized epithelial cells (Dotti and Simons, 1990; Jareb and Banker, 1998; Rongo et al., 1998). To determine whether this parallel also applies to sorting of a palmitoylated postsynaptic protein, we evaluated localization of stably transfected PSD-95 in polarized MDCK cells. Indeed, we found that full-length PSD-95 colocalizes with E-cadherin at the basolateral membrane (Fig. 6 A, left), but not with the apical marker gp-135 (Fig. 6 A, right). To determine whether palmitoylation is essential for basolateral membrane sorting, we examined the localization of various mutants. Strikingly, all point mutations of PSD-95 that disrupt palmitoylation (Cys3Leu, Leu4Ala, Leu4Ser, Cys5Leu, and Ile6Ser) also block its lateral membrane sorting (Fig. 6 C). In contrast, PSD-95 occurs at the lateral membrane in transfections with a mutant that retains its palmitoylation (Ile6Leu).

To determine the domains of PSD-95 that, together with the palmitoylated NH_2 terminus, mediate basolateral localization, two stably transfected MDCK cell lines were

generated that express increasingly longer NH_2-terminal constructs of PSD-95. The first line, containing the NH_2 terminus and the first PDZ domain (1-PDZ1) occurs diffusely in the cells whereas the second line, containing the NH_2 terminus and the 3 PDZ domains (1-PDZ3) is polarized to the basolateral surface, just like full-length PSD-95 (Fig. 6 B). These experiments indicate that basolateral membrane targeting requires not only the palmitoylated NH_2 terminus but also the PDZ domains. On the other hand, the SH3 and guanylate kinase regions are not required. It is important to note that, in sub-confluent cultures, palmitoylated PSD-95 constructs colocalize with M6PR positive vesicles whereas mutants that disrupt palmitoylation are expressed diffusely in nonconfluent MDCK cells (data not shown). Taken together, these data indicate that basolateral membrane targeting of PSD-95 requires both palmitoylation and PDZ domain interactions.

Postsynaptic Targeting of PSD-95 Requires Dual Palmitoylation

To evaluate the role of dual palmitoylation in postsynaptic sorting of PSD-95, we evaluated targeting of a series of NH_2-terminal mutants in primary hippocampal neurons (at DIV 12). We found that dually palmitoylated constructs (wild-type, Thr8,9Ala, Ile6Leu and Val7Leu) all target appropriately to postsynaptic dendritic clusters (Fig.

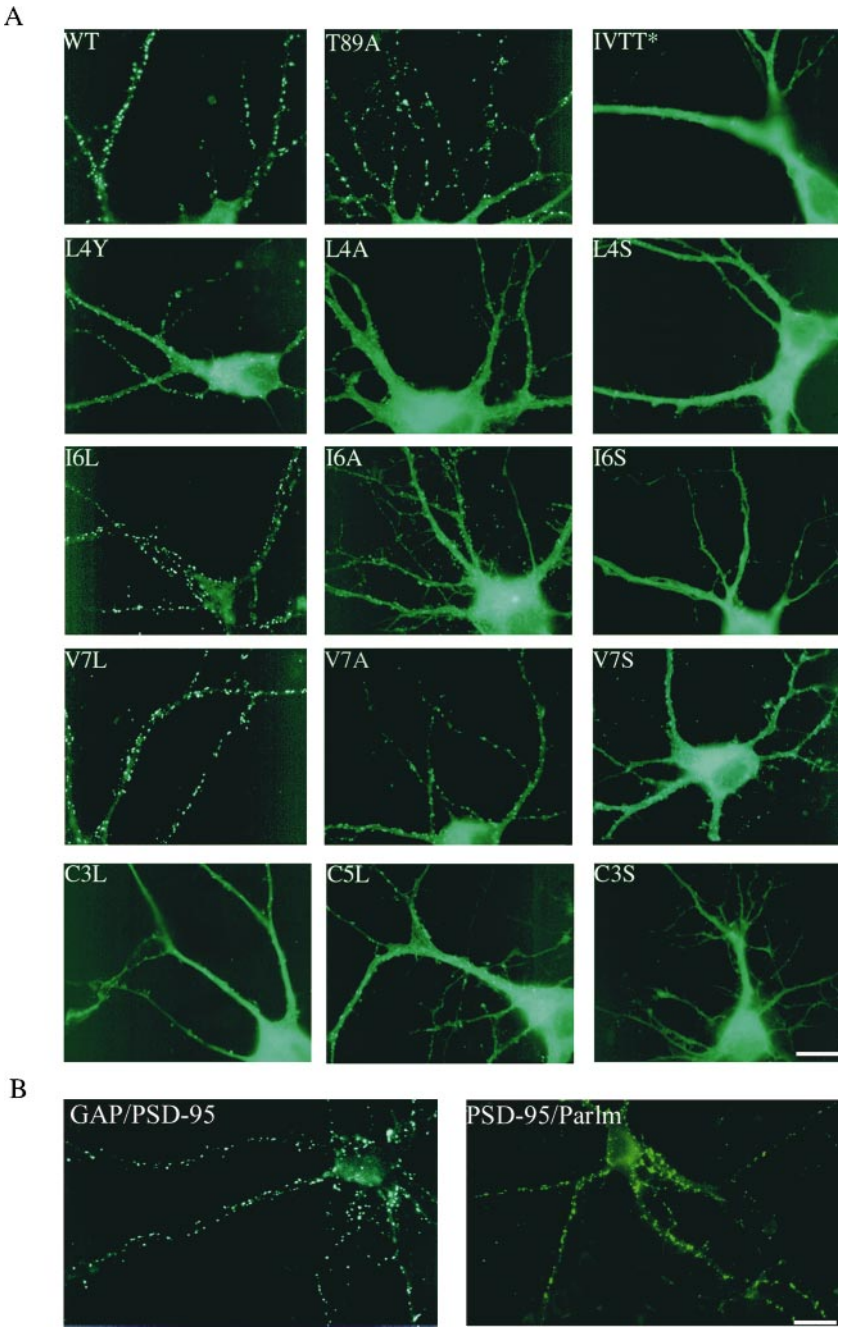

Figure 7. Postsynaptic targeting of PSD-95 in hippocampal neurons requires the NH_2-terminal dually palmitoylated motif. (A) Mutations that block PSD-95 palmitoylation (IVTT to TEIN; IVTT*, L4S, I6S) also disrupt postsynaptic targeting of PSD-95. In contrast, mutations that do not disrupt palmitoylation of PSD-95 (I6L, V7L, and T89A) do not alter its postsynaptic targeting. Mutations that reduce palmitoylation (L4Y, L4A, I6A, V7A, and V7S) result in inefficient targeting of PSD-95 to postsynaptic sites. Mutation of Cys3 to Ser (C3S) abolishes protein palmitoylation and synaptic targeting. In contrast, mutations of either Cys to Leu (C3L, C5L), which partially preserve protein palmitoylation, result in very inefficient synaptic targeting. (B) A chimera containing the first 12 amino acids of GAP-43 fused to PSD-95 (GAP/PSD-95) is targeted to postsynaptic sites. The COOH-terminal 12–amino acid palmitoylated motif of paralemmin fused to PSD-95:C3,5S (PSD-95/Parlm) induces postsynaptic clustering of a PSD-95 (C3,5S) mutant. Bar, 10 μm.

7 A). By contrast, all nonpalmitoylated constructs occur diffusely in dendrites of transfected neurons (Cys3Ser, Leu4Ser, and Ile6Ser). Constructs that show reduced palmitoylation (Leu4Tyr, Leu4Ala, Cys3Leu, Cys5Leu, Ile6Ala, Val7Ala, and Val7Ser) are partially clustered in neurons (Fig. 7 A). The lack of proper sorting of the Cys3Leu and Cys5Leu constructs, which are singly palmitoylated, suggests that there is a fundamental difference between single and dual palmitoylation and that postsynaptic targeting requires dual palmitoylation. Furthermore, adding the NH_2-terminal dually palmitoylated motif of GAP-43 or the COOH-terminal prenylated and dually palmitoylated motif of paralemmin to PSD-95(C3,5S) significantly restore postsynaptic targeting. With the GAP-43 motif and the paralemmin motif PSD-95 clusters form in 46 and 81% of neurons, whereas only 22% of cells show clusters without these motifs (Fig. 7 B).

Ion Channel Clustering by PSD-95 Requires Dual Palmitoylation

Certain aspects of channel clustering by MAGUK proteins can be reproduced in a coclustering experiment in heterologous cells (Kim et al., 1995). In this assay, cotransfection of PSD-95 with Shaker K^+ channel Kv1.4 causes a striking redistribution of both proteins to raft-like clusters on the cell surface (Fig. 8 A, top). We used video microscopy to monitor the dynamics of this cluster formation in live cells transfected with PSD-95 GFP and Kv1.4 (see video 5). In cells cotransfected with PSD-95 GFP and Kv1.4, the surface patches appear to derive from dynamic vesiculotubular transport intermediates for PSD-95 that undergo dramatic shape changes and fuse with the plasma (see videos 5–7).

To define the role for dual palmitoylation in ion channel clustering we analyzed a series of PSD-95 mutants. We found that mutants of PSD-95 that disrupt palmitoylation, including L4S, I6S, C3S, and C35S, do not form coclustered membrane patches when coexpressed with Kv1.4 (Fig. 8 A, top and lower right panels and data not shown). In contrast, mutants of PSD-95 that do not disrupt palmitoylation of PSD-95 including I6L and V7L coclustered with Kv1.4 (Fig. 8 A, and data not shown). Furthermore, the NH_2-terminal palmitoylated motif of GAP-43 or the COOH-terminal palmitoylated motif of paralemmin can functionally substitute for the PSD-95 NH_2 terminus to mediate ion channel clustering (Fig. 8 B).

Finally, minimal constructs of PSD-95 were designed to define the absolute requirements for ion channel clustering. Kv1.4 clustering is induced by the expression of a construct containing only the first 26 amino acids of PSD-95 fused to PDZ domains 1 and 2. In addition, a construct

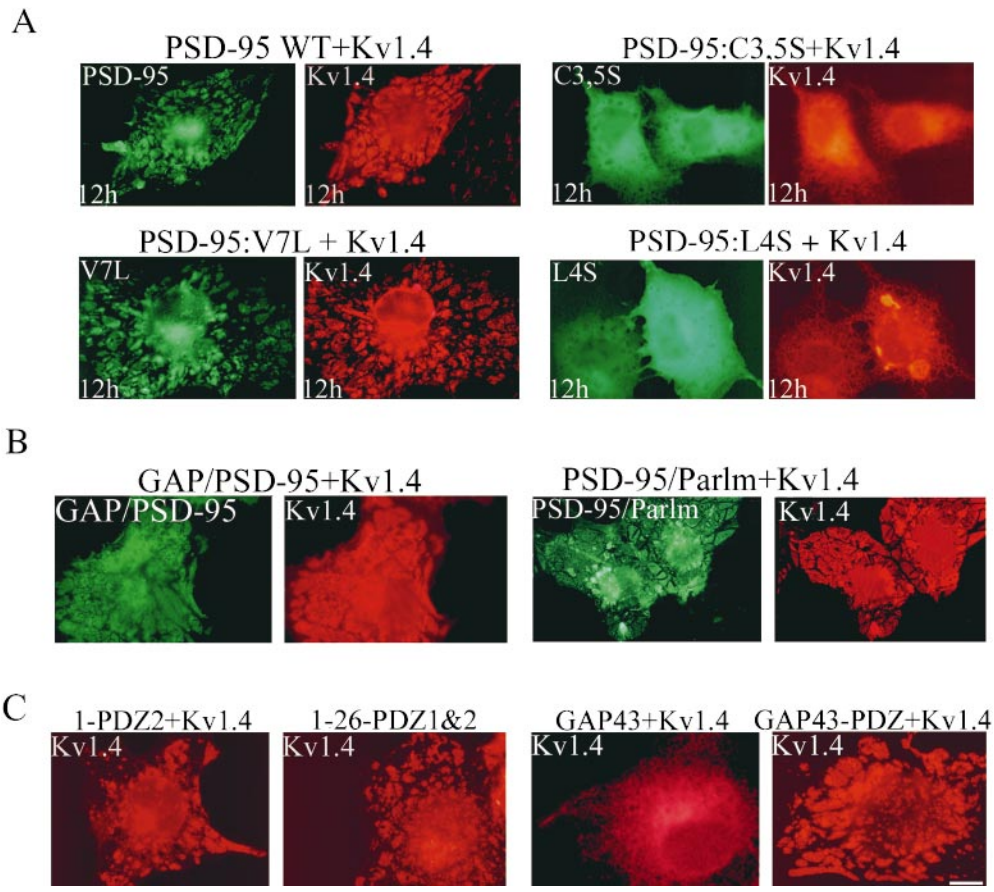

Figure 8. Ion channel clustering requires dual palmitoylation of PSD-95. COS cells were cotransfected with Kv1.4 and wild-type or mutant forms of PSD-95 (C3,5S, V7L, or L4S). Cells were fixed 12 h (12h) after transfection and double-labeled with antibodies to PSD-95 (green) and Kv1.4 (red). Palmitoylation-deficient mutants of PSD-95 (C3,5S, or L4S) block clustering whereas the palmitoylated mutant (V7L) functions normally. (B) Chimeras containing the first 12 amino acids of GAP-43 fused to PSD-95 (GAP/PSD-95) or the last 12 amino acids of paralemmin fused to PSD-95 C3,5S (PSD-95/Parlm) mediate clustering of Kv1.4. (C) Cotransfection of Kv1.4 with a construct containing either the first 300 amino acids of PSD-95 (1-PDZ2) or amino acids 1-26 fused to PDZ1&2 (1-26-PDZ1&2) are sufficient for clustering Kv1.4. A construct containing full-length GAP-43 fused to PDZ domains 1 and 2 (GAP43-PDZ) but not GAP-43 itself also induces channel clustering. Bar, 10 μm.

containing GAP-43, fused to only PDZ domains 1&2 of PSD-95 is capable of clustering Kv1.4 (Fig. 8 C). These experiments establish that ion channel clustering by PSD-95 requires (a) dual palmitoylation and (b) an appropriate PDZ domain.

Discussion

This work demonstrates that dual palmitoylation of PSD-95 mediates a transient association with perinuclear vesicles and that this lipid modification is also essential for ion channel clustering and postsynaptic targeting. Dual palmitoylation of PSD-95 is determined by a consensus sequence of five consecutive NH_2-terminal hydrophobic amino acids that include the two modified cysteines. Importantly, all mutations that disrupt dual palmitoylation block perinuclear trafficking, postsynaptic targeting, and ion channel clustering activity of PSD-95.

Synaptic Targeting and Ion Channel Clustering by PSD-95 Require Dual Palmitoylation

This work emphasizes the central role for NH_2-terminal palmitoylation in protein sorting by PSD-95. Previous studies noted essential roles for cysteines 3 and 5 in both receptor clustering (Hsueh et al., 1997) and postsynaptic targeting of PSD-95 (Craven et al., 1999). Although these cysteines were identified as sites of palmitoylation (Topinka and Bredt, 1998), it was unclear how this lipid modification participates in synaptic clustering. Several lines of evidence developed here indicate that palmitoylation may mediate ion channel clustering by initially targeting PSD-95 to the cytosolic surface of intracellular vesicles. First, video microscopy suggests that vesiculotubular structures are transport intermediates for coclustering of PSD-95 and Kv1.4 in heterologous cells. Second, localization of PSD-95 to perinuclear vesicles in heterologous cells and developing neurons requires an NH_2-terminal consensus that supports dual palmitoylation. Third, those mutations that disrupt sorting of PSD-95 to the perinuclear domain prevent both ion channel clustering in heterologous cells and postsynaptic sorting in neurons. In addition, the palmitoylated NH_2 terminus of PSD-95 can functionally be replaced with other NH_2- or COOH-terminal palmitoylation motifs to mediate ion channel clustering or postsynaptic targeting. Although these mutagenesis experiments can provide only indirect evidence, they do demonstrate a strict correlation between vesiculotubular trafficking and receptor clustering by PSD-95. Taken together, these results support a role for vesicular trafficking in sorting and clustering of PSD-95 at synaptic sites.

Five Consecutive Hydrophobic Amino Acids Specifies Palmitoylation of PSD-95

Our detailed mutagenesis of the NH_2 terminus of PSD-95 demonstrates that a sequence of five consecutive hydrophobic amino acids (containing the two modified cysteines) is essential for palmitoylation. Conservative mutations of any of these five amino acids (including the cysteines) to other hydrophobic amino acids preserve palmitoylation whereas mutations to a hydrophilic amino acid prevent palmitoylation. Interestingly, palmitoylation of GAP-43 is also specified by five consecutive NH_2-terminal hydrophobic amino acids that otherwise shares no similarity with the sequence of PSD-95.

Despite the central role for palmitoylation in diverse cellular processes, the identity of the putative palmitoyltransferase enzyme remains mysterious. Our identification of a strict consensus sequence in PSD-95 and GAP-43 for palmitoylation strongly suggests that modifications of these proteins are enzyme-mediated. Similar to what is found for protein kinases, the PAT appears to recognize a short consensus sequence. Because PSD-95 is such a potent substrate for PAT, the NH_2 terminus of PSD-95 may be a useful tool for biochemical characterization and isolation of this important and elusive enzyme.

Comparison of Postsynaptic Clustering with Basolateral Membrane Sorting

That postsynaptic clustering in neurons and basolateral membrane targeting in epithelial cells both require palmitoylation of PSD-95 suggests interesting parallels between these pathways. Previous analyses of trafficking of transmembrane proteins in epithelial cells have identified critical protein and lipid modifications that mediate polarized protein sorting. Basolateral sorting of several transmembrane proteins is determined by short cytoplasmic tyrosine or dileucine based motifs (Trowbridge et al., 1993) that interact with clathrin adaptor proteins, consistent with roles for endocytosis, transcytosis and vesicular budding in basolateral protein sorting (Ohno et al., 1995). Our data imply that vesicular trafficking may play a role in basolateral membrane localization of a palmitoylated protein in polarized epithelial cells. In addition to palmitoylation, PDZ domains are also essential for lateral membrane targeting. This is consistent with recent work showing that PDZ domains of SAP-97 are important for its lateral membrane localization (Wu et al., 1998). One major difference is that postsynaptic targeting of PSD-95 requires a short COOH-terminal sorting motif (Craven et al., 1999) that we find is dispensable for basolateral membrane localization.

Implications for Synaptic Plasticity Regulated by MAGUK Proteins

Mice with mutant PSD-95 protein have a dramatic shift in NMDA receptor-dependent plasticity in hippocampus such that long-term depression (LTD) is blocked and long-term potentiation (LTP) is enhanced (Migaud et al., 1998). These abnormalities in synaptic plasticity presumably explain why the mutant mice are impaired in a spatial learning task. As postsynaptic signaling cascades downstream of NMDA receptors play critical roles in LTP and LTD, it seems likely that PSD-95 plays an essential role in linking NMDA receptors to these pathways.

How PSD-95 assembles these signaling complexes, however, remains uncertain. Previous models, based on the assumption that PSD-95 and other MAGUKs are static elements of the postsynaptic cytoskeleton suggested a passive role for these proteins in simply retaining receptor clusters and associated signaling enzymes at the synapse (Zito et al., 1997). The trafficking of PSD-95 with vesiculotubular intermediates here suggests an alternative mechanism, inter-

action of PSD-95 with the cytosolic tails of receptors residing in intracellular vesicles followed by insertion of these ion channel complexes into the plasma membrane. Such a model for interaction of PSD-95 with ion channels in sorting endosomes provides a mechanism to help explain recent work showing that PSD-95 regulates polarized trafficking of Kv1.4 (Arnold and Clapham, 1999). Interestingly, recent work suggests that other multi-PDZ domain proteins involved in synaptic organization including the glutamate interacting protein (GRIP) and LIN-10 also associate with post-Golgi vesicles (Rongo et al., 1998; Xia et al., 1999). This may indicate a common role for PDZ proteins in transport of receptor-containing vesicles. Such a dynamic mechanism would allow for precise and regulated assembly of synaptic transduction machinery.

We thank Alice Elste for excellent technical assistance with electron microscopy, Yorum Altschuler for help with confocal microscopy and Robert Edwards and Keith Mostov for critically reviewing the manuscript.

This work was supported by a pre-doctoral research grant from the National Science Foundation and an ARCS Foundation scholarship (to S.E. Craven), and postdoctoral grants from the Medical Research Council of Canada (to A.E. El-Husseini), the National Institute of Child Health and Development and Spinal Cord Research Foundation (to B.L. Firestein), and the Howard Hughes Medical Institute (to D.M. Chetkovich). This research was also supported by grants (to C. Aoki) from the National Institutes of Health (R01-EY08055), NSF (RCD 92-53750), NYU Research Challenge Fund, and Human Frontier's Science Program Award and by grants (to D.S. Bredt) from the National Institutes of Health (R01-NS36017), National Science Foundation, the National Association for Research on Schizophrenia and Depression, the EJLB, and the Culpeper and Beckman Foundations.

Submitted: 6 October 1999
Revised: 29 November 1999
Accepted: 1 December 1999

References

Aoki, C., D.S. Bredt, S. Fenstemaker, and M. Lubin. 1998. The subcellular distribution of nitric oxide synthase relative to the NR1 subunit of NMDA receptors in the cerebral cortex. *Prog. Brain Research*. 118:83–97.

Aoki, C., H. Oviedo, L. Alexandre, and D.S. Bredt. 1999a. Synaptic membranous and cytoplasmic localization of PSD-95: EM-immunocytochemical detection with intact developing cortical neuropil. *Soc. Neurosci. Abstr*. 510.8: 1277.

Aoki, C., S. Rodrigues, and H. Kurose. 1999b. Use of electron microscopy in the detection of adrenergic receptors. *In* Methods in Molecular Biology: Adrenergic Receptor Protocols. C.M. Machinda, editor. Humana Press. 535–563.

Arnold, D.B., and D.E. Clapham. 1999. Molecular determinants for subcellular localization of PSD-95 with an interacting K+ channel. *Neuron*. 23:149–157.

Brenman, J.E., D.S. Chao, S.H. Gee, A.W. McGee, S.E. Craven, D.R. Santillano, F. Huang, H. Xia, M.F. Peters, S.C. Froehner, and D.S. Bredt. 1996a. Interaction of nitric oxide synthase with the postsynaptic density protein PSD-95 and α-1 syntrophin mediated by PDZ motifs. *Cell*. 84:757–767.

Brenman, J.E., K.S. Christopherson, S.E. Craven, A.W. McGee, and D.S. Bredt. 1996b. Cloning and characterization of postsynaptic density 93 (PSD-93), a nitric oxide synthase interacting protein. *J. Neurosci.* 16:7407–7415.

Chan, J., C. Aoki, and V.M. Pickel. 1990. Optimization of differential immunogold-silver and peroxidase labeling with maintenance of ultrastructure in brain sections before plastic embedding. *J. Neurosci. Methods.* 33:113–127.

Cho, K.O., C.A. Hunt, and M.B. Kennedy. 1992. The rat brain postsynaptic density fraction contains a homolog of the *Drosophila* discs-large tumor suppressor protein. *Neuron*. 9:929–942.

Cole, N.B., N. Sciaky, A. Marotta, J. Song, and J. Lippincott-Schwartz. 1996. Golgi dispersal during microtubule disruption: regeneration of Golgi stacks at peripheral endoplasmic reticulum exit sites. *Mol. Biol. Cell*. 7:631–650.

Craven, S.E., and D.S. Bredt. 1998. PDZ proteins organize synaptic signaling pathways. *Cell*. 93:495–498.

Craven, S.E., A.E. El-Husseini, and D.S. Bredt. 1999. Synaptic targeting of the postsynaptic density protein PSD-95 mediated by lipid and protein motifs. *Neuron*. 22:497–509.

Dotti, C.G., and K. Simons. 1990. Polarized sorting of viral glycoproteins to the axon and dendrites of hippocampal neurons in culture. *Cell*. 62:63–72.

Griffiths, G., B. Hoflack, K. Simons, I. Mellman, and S. Kornfeld. 1988. The mannose 6-phosphate receptor and the biogenesis of lysosomes. *Cell*. 52: 329–341.

Hsueh, Y.P., E. Kim, and M. Sheng. 1997. Disulfide-linked head-to-head multimerization in the mechanism of ion channel clustering by PSD-95. *Neuron*. 18:803–814.

Hunt, A.C., L.J. Schenker, and M.B. Kennedy. 1996. PSD-95 is associated with the postsynaptic density and not with the presynaptic membrane at forebrain synapses. *J. Neurosci.* 16:1380–1388.

Jareb, M., and G. Banker. 1998. The polarized sorting of membrane proteins expressed in cultured hippocampal neurons using viral vectors. *Neuron*. 20: 855–867.

Kennedy, M.B. 1998. Signal transduction molecules at the glutamatergic postsynaptic membrane. *Brain Res. Rev*. 26:243–257.

Kim, E., M. Niethammer, A. Rothschild, Y.N. Jan, and M. Sheng. 1995. Clustering of Shaker-type K+ channels by direct interaction with the PSD-95/SAP90 family of membrane-associated guanylate kinases. *Nature*. 378:85–88.

Kistner, U., B.M. Wenzel, R.W. Veh, C. Cases-Langhoff, A.M. Garner, U. Appeltauer, B. Voss, E.D. Gundelfinger, and C.C. Garner. 1993. SAP90, a rat presynaptic protein related to the product of the *Drosophila* tumor suppressor gene dlg-A. *J. Biol Chem*. 268:4580–4583.

Kornau, H.-C., L.T. Schenker, M.B. Kennedy, and P.H. Seeburg. 1995. Domain interaction between NMDA receptor subunits and the postsynaptic density protein PSD-95. *Science*. 269:1737–1740.

Kornau, H.-C., P.H. Seeburg, and M.B. Kennedy. 1997. Interaction of ion channels and receptors with PDZ domains. *Curr. Opin. Neurobiol.* 7:368–373.

Kutzleb, C., G. Sanders, R. Yamamoto, X. Wang, B. Lichte, E. Petrasch-Parwez, and M.W. Kilimann. 1998. Paralemmin, a prenyl-palmitoyl-anchored phosphoprotein abundant in neurons and implicated in plasma membrane dynamics and cell process formation. *J. Cell Biol.* 143:795–813.

Lippincott-Schwartz, J., L. Yuan, C. Tipper, M. Amherdt, L. Orci, and R.D. Klausner. 1991. Brefeldin A's effects on endosomes, lysosomes, and the TGN suggest a general mechanism for regulating organelle structure and membrane traffic. *Cell*. 67:601–616.

Liu, Y., D.A. Fisher, and D.R. Storm. 1993. Analysis of the palmitoylation and membrane targeting domain of neuromodulin (GAP-43) by site-specific mutagenesis. *Biochemistry*. 32:10714–10719.

Migaud, M., P. Charlesworth, M. Dempster, L.C. Webster, A.M. Watabe, M. Makhinson, Y. He, M.F. Ramsay, R.G. Morris, J.H. Morrison, T.J. O'Dell, and S.G. Grant. 1998. Enhanced long-term potentiation and impaired learning in mice with mutant postsynaptic density-95 protein. *Nature*. 396:433–439.

Ohno, H., J. Stewart, M.C. Fournier, H. Bosshart, I. Rhee, S. Miyatake, T. Saito, A. Gallusser, T. Kirchhausen, and J.S. Bonifacino. 1995. Interaction of tyrosine-based sorting signals with clathrin-associated proteins. *Science*. 269: 1872–1875.

Rongo, C., C.W. Whitfield, A. Rodal, S.K. Kim, and J.M. Kaplan. 1998. LIN-10 is a shared component of the polarized protein localization pathways in neurons and epithelia. *Cell*. 94:751–759.

Sciaky, N., J. Presley, C. Smith, K.J. Zaal, N. Cole, J.E. Moreira, M. Terasaki, E. Siggia, and J. Lippincott-Schwartz. 1997. Golgi tubule traffic and the effects of brefeldin A visualized in living cells. *J. Cell Biol*. 139:1137–1155.

Sheng, M., and M. Wyszynski. 1997. Ion channel targeting in neurons. *Bioessays*. 19:847–853.

Tejedor, F.J., A. Bokhari, O. Rogero, M. Gorczyca, J. Zhang, E. Kim, M. Sheng, and V. Budnik. 1997. Essential role for dlg in synaptic clustering of Shaker K+ channels in vivo. *J. Neurosci.* 17:152–159.

Topinka, J.R., and D.S. Bredt. 1998. N-terminal palmitoylation of PSD-95 regulates association with cell membranes and interaction with K+ channel, Kv1.4. *Neuron*. 20:125–134.

Trowbridge, I.S., J.F. Collawn, and C.R. Hopkins. 1993. Signal-dependent membrane protein trafficking in the endocytic pathway. *Annu. Rev. Cell Biol.* 9:129–161.

Valtschanoff, J.G., A. Burette, R.J. Wenthold, and R.J. Weinberg. 1999. Expression of NR2 receptor subunit in rat somatic sensory cortex: synaptic distribution and colocalization with NR1 and PSD-95. *J. Comp. Neurol.* 410: 599–611.

Wu, H., S.M. Reuver, S. Kuhlendahl, W.J. Chung, and C.C. Garner. 1998. Subcellular targeting and cytoskeletal attachment of SAP97 to the epithelial lateral membrane. *J. Cell Sci.* 111:2365–2376.

Xia, J., X. Zhang, J. Staudinger, and R.L. Huganir. 1999. Clustering of AMPA Receptors by the synaptic PDZ domain-containing protein PICK1. *Neuron*. 22:179–187.

Zito, K., R.D. Fetter, C.S. Goodman, and E.Y. Isacoff. 1997. Synaptic clustering of Fascilin II and Shaker: essential targeting sequences and role of Dlg. *Neuron*. 19:1007–1016.